Wideband Phase Modulator MMIC for K-Band Supply-Modulated Power Amplifier Linearization

Gregor Lasser[#1], Connor Nogales[#2], Maxwell R. Duffy[*3], Zoya Popović[#4]
[#]Univ. of Colorado, Boulder, USA
[*]Northrop Grumman, Redondo Beach, USA
{[1]gregor.lasser, [2]connor.nogales, [4]zoya}@colorado.edu, [3]duffy.mr@gmail.com

***Abstract*— A GaAs MMIC phase modulator with an RF bandwidth from 15 to 30 GHz and a modulation bandwidth of dc to 1 GHz is described. The phase modulator is designed for supply-modulated power amplifier linearization, and its dynamic modulation performance is characterized. From 15 to 25 GHz the circuit achieves a frequency-stable peak phase variation of $(42 \pm 2)^\circ$ for modulation signals with instantaneous bandwidths ranging from dc to 50 MHz, with an insertion loss below 3.2 dB.**

***Keywords*— phase modulation, phase shifter, linearization**

I. Introduction

Supply modulation is a well established approach for improving efficiency of power amplifiers (PAs) in backoff [1], that typically comes at the expense of degraded linearity since the PA operates in or close to compression. Even at lower signal levels below compression, the gain amplitude and phase of a PA are dependent on the supply voltage [1] which creates distortion. While the mainstream approach to linearization is digital predistortion, analog linearization has its place where digital baseband processing is not feasible. This is the case, e.g., in repeaters where the baseband is not known, when the signal bandwidth is excessive [2], or the added complexity is prohibitive e.g. for phased arrays [3].

In this work we describe a phase modulator that is suitable for phase linearization [4], [5] of a supply modulated PA as shown in Fig. 1a. The RF input signal is first routed through a phase modulator, that is directly controlled by the time varying supply voltage $V_\mathrm{D}(t)$, appropriately scaled through a signal conditioning network. This network adapts the drain voltage swing to the modulation voltage required by the phase modulator, and in its simplest form is just a resistive voltage divider. When the sign and magnitude of the phase modulation introduced by the modulator are chosen appropriately, they cancel the phase modulation introduced by the PA when supply-modulated, hence improving the overall linearity.

We first discuss the phase distortions introduced by amplitude and drain voltage variations in a K-band MMIC PA. This motivates the design of a phase modulator MMIC implemented in the WIN Semiconductor PIH1-10 enhancement mode GaAs pHEMT process [6]. We further characterize the phase modulator in terms of its static S-parameters at the RF ports, as well as at the modulation port. To explore the usability as a phase modulator for wideband signals, the dynamic modulation performance in terms of stability of the peak phase variation from 250 kHz up to 1 GHz is characterized. We also demonstrate the modulation purity of the circuit in terms of the demodulated harmonics.

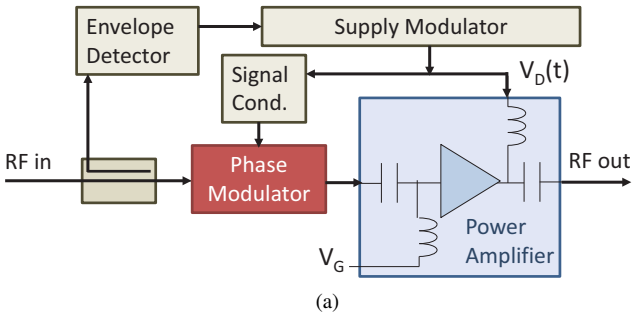

(a)

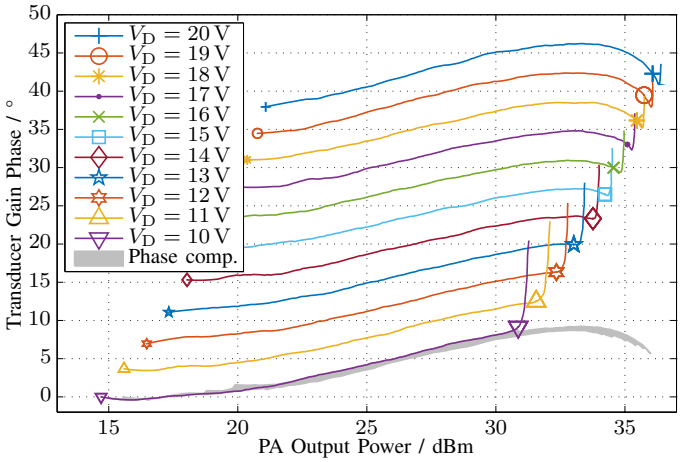

(b)

Fig. 1. The phase modulator as a linearizer for a supply modulated PA (a); Transducer gain phase of K-band MMIC PA [7] for different supply voltages measured at 19.8 GHz (b). The large markers to the right indicate the peak PAE points. The shaded grey area (Phase comp.) indicates the phase variation when the phases for drain voltages $V_\mathrm{D} > 10\,\mathrm{V}$ are shifted by $-3.7\,^\circ/\mathrm{V}$.

II. Phase Distortion of Supply-Modulated PAs

When the supply voltage of a PA is varied, the magnitude and phase of the transducer gain vary as well [8]. This implies that supply modulation inherently introduces phase distortion, which is particularly noticeable for discrete supply modulation [9], [10]. Fig. 1b shows the phase of the transducer gain of a three-stage K-band MMIC PA in 150 nm GaN technology [7] measured for different output powers using a vector network

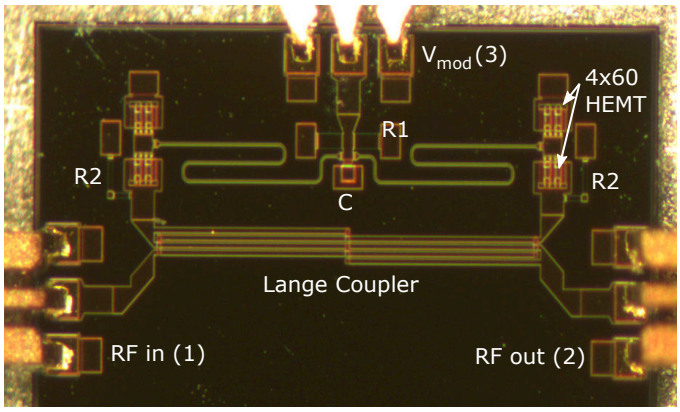

(a)

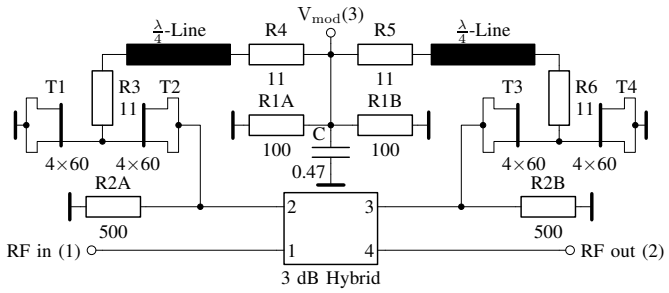

(b)

Fig. 2. Chip photograph (a) and schematic (b) of the phase modulator GaAs MMIC measuring $0.95 \times 1.985\,\mathrm{mm}^2$. The numbers (1,2,3) correspond to the port designations used throughout the paper. All capacitor values are in pf, all resistors are in Ω, transistor periphery sizes are given in fingers × gate width in µm.

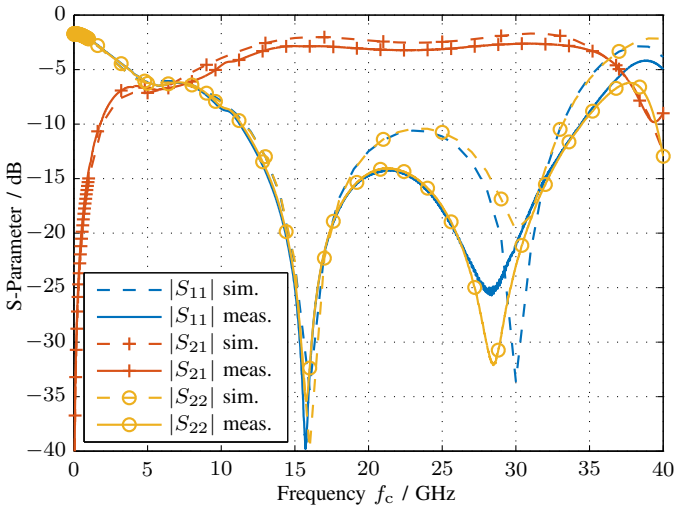

Fig. 3. Simulated and measured S-parameters for a bias voltage $V_\mathrm{b} = 0.35\,\mathrm{V}$.

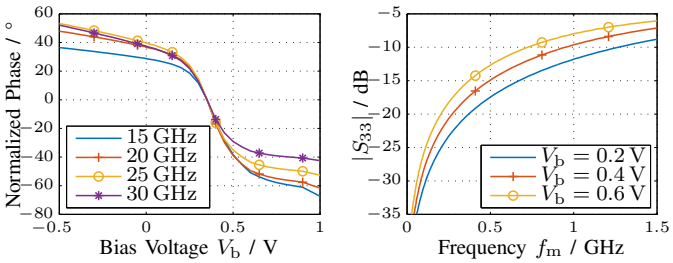

(a) (b)

Fig. 4. Measured normalized phase shift across the band for a dc bias sweep (a), modulation port (3) reflection coefficient for different dc bias voltages (b).

analyzer. The phase is normalized to the minimum-power, 10 V point. The drain voltage of the first stage is fixed at 20 V, while the drain supply voltages of the remaining stages jointly vary between 10 V and 20 V. The large markers to the right indicate the power level for maximum power-added efficiency (PAE) for each drain voltage. For all measured static supply voltages, the phase from the minimum power to the maximum-PAE power level varies at most 9°. Ignoring thermal and memory effects, the predicted amplitude-to-phase distortion is also 9° for the static supply voltage case. When this PA is supply modulated for efficiency enhancement, the full range up to the maximum PAE points is traversed, resulting in significantly increased amplitude-to-phase distortion of about 40°. However, the extra phase shift introduced by the supply modulation is practically constant across output powers, and is approximately $3.7\,°/\mathrm{V}$. Therefore, a phase modulator that provides $-3.7\,°/\mathrm{V}$ of phase shift compensates this phase distortion, as shown by the shaded area in Fig. 1b.

III. Circuit Description

The phase modulator MMIC is based on the reflection-type phase shifter incorporating a 90°-hybrid coupler [11]. In contrast to a phase shifter where a phase range of 360° is typically required, this phase modulator is designed for the K-band MMIC PA described above, and 40° of phase shift is sufficient for phase compensation (Fig. 1b). In this phase linearization application the phase modulation signal $V_\mathrm{m}(t)$ is derived from the envelope of the transmit signal and hence has a bandwidth that is approximately five times as large as the original signal bandwidth [1]. This means that for a modulation bandwidth of 200 MHz the modulation signal will have a bandwidth of dc to 1 GHz and thus a modulation port with stable termination impedance is desirable to archive a flat frequency response. This demands a wideband bias line design not required for regular phase shifters.

The phase modulator MMIC is shown in Fig. 2 and uses a 4-arm Lange coupler for the 90°-hybrid. The variable reflective loads are formed by the gate Schottky junctions of $4 \times 60\,\mu\mathrm{m}$ HEMTs, with shorted drain and source terminals. The reactances on the two ports of the Lange coupler consist of two Schottky diodes connected in anti-series to ground.

The anti-series connection reduces nonlinear distortion due to self-modulation of the diode capacitance by the RF signal. In parallel to the diodes, the respective coupler ports are also connected to ground through 500 Ω resistors R2, providing a dc return path for the bottom diode and reducing the insertion loss variation for different phase settings. The anodes of the two diodes (the common gate contacts) are biased through high-impedance quarter-wavelength transformers that are connected in the center of the chip and terminated by a

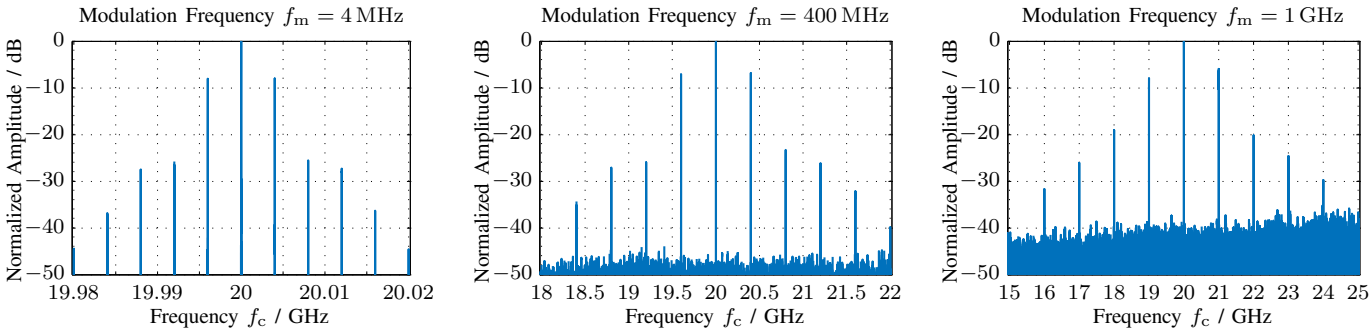

Fig. 5. Spectra obtained by observing the modulated carrier at $f_\mathrm{c} = 20\,\mathrm{GHz}$ using a sinusoidal modulation signal with power $P_\mathrm{m} = -5\,\mathrm{dBm}$. The modulation frequencies are $4\,\mathrm{MHz}$ (a), $400\,\mathrm{MHz}$ (b), $1\,\mathrm{GHz}$ (c). The span is adjusted to plot modulation components up to order $N = 5$.

$0.47\,\mathrm{pF}$ bypass capacitor C and two parallel $100\,\Omega$ resistors R1(A&B). These resistors create a $50\,\Omega$ termination for the modulation signal port. Each end of the quarter-wavelength bias lines additionally contains a $11\,\Omega$ series resistor (R3-R6 in Fig. 2b) to improve the wideband performance.

IV. Static RF Performance

RF performance of the phase modulator MMIC was evaluated on wafer with a vector network analyzer calibrated using on-wafer standards. The S-parameters were evaluated for a bias voltage sweep from $0.2\,\mathrm{V}$ to $0.5\,\mathrm{V}$, where the insertion loss between 14 and $22\,\mathrm{GHz}$ varies less than $0.5\,\mathrm{dB}$ and the maximum variation across the band is $0.61\,\mathrm{dB}$ at $27\,\mathrm{GHz}$. A comparison of simulated and measured S-parameters when a static bias voltage of $V_\mathrm{b} = 0.35\,\mathrm{V}$ is applied to the modulation port is shown in Fig. 3. This bias voltage is chosen because it is approximately in the center of the tuning range as discussed next. The measured insertion loss at $15\,\mathrm{GHz}$ and $20\,\mathrm{GHz}$ is $2.85\,\mathrm{dB}$ and $3.1\,\mathrm{dB}$, respectively, which is $0.8\,\mathrm{dB}$ higher than simulated. The measured return loss is better than simulated, and remains above $10\,\mathrm{dB}$ from 13 to $34\,\mathrm{GHz}$.

The static phase modulation capabilities of the MMIC phase modulator are shown in Fig. 4a, where the phase is normalized to zero for $V_\mathrm{b} = 0.35\,\mathrm{V}$ at each frequency. While the total phase shift exceeds $100°$, a linear phase vs. bias voltage is realized across a $40°$ span, centered around $V_\mathrm{b} = 0.375\,\mathrm{V}$, which was chosen as the dc bias voltage for subsequent dynamic measurements. The reflection coefficient at the modulation port is plotted in Fig. 4b and remains lower than $-8\,\mathrm{dB}$ from dc to $1\,\mathrm{GHz}$, even for an extreme modulation bias of $V_\mathrm{b} = 0.6\,\mathrm{V}$ where the diode connected FETs start to conduct. Below $V_\mathrm{b} = 0.6\,\mathrm{V}$ the bias current is negligible.

V. Dynamic Modulation Performance

A continuous wave (CW) carrier at frequency f_c is input to the phase modulator to evaluate the bandwidth and linearity in terms of the modulated signal fidelity. The output is observed with a vector signal analyzer (VSA), while the modulation port is fed by a separate RF generator through a bias-T to create the sinusoidal modulated signal

$$V_\mathrm{m}(t) = V_\mathrm{b} + \hat{V}_\mathrm{m} \sin(2\pi f_\mathrm{m} t) \tag{1}$$

with dc bias voltage offset V_b, modulation peak amplitude $\hat{V}_\mathrm{m}$, and modulation frequency f_m. For the following measurements we set the dc bias voltage to $V_\mathrm{b} = 0.375\,\mathrm{V}$, which lays in the center of the linear range of Fig. 4a for $20\,\mathrm{GHz}$. The power at the modulation port was calibrated using a power sensor to account for the cable losses.

A sinusoidally phase-modulated signal spectrum can be described by [12, (2.49)]

$$S(f) \sim \sum_{n=-\infty}^{\infty} J_n(\beta)\big(\delta(f - f_\mathrm{c} - n f_\mathrm{m}) + \delta(f + f_\mathrm{c} + n f_\mathrm{m})\big), \tag{2}$$

where J_n is the Bessel function of first kind, δ is the Dirac delta function, and β is the modulation index which for phase modulation is simply the maximum phase variation $\beta = \Delta\varphi$. This means that the phase modulated spectrum contains discrete lines spaced by a multiple of the modulation frequency f_m, and their amplitude ratio to the carrier $\frac{J_n(\beta)}{J_0(\beta)}$ defines the modulation index. For an ideal phase modulator the modulation index is proportional to the modulation peak amplitude $\beta \sim \hat{V}_\mathrm{m}$.

Fig. 5 shows the resulting normalized spectra at $f_\mathrm{c} = 20\,\mathrm{GHz}$ for three different modulation frequencies. Note that the frequency axes are scaled differently, and the resolution bandwidths are adapted as well to capture the spectra without gaps using the available 40001 points of the VSA, which results in the increase of the noise floor for Fig. 5c. We observe that the amplitudes of the spectral lines remain relatively constant over frequency, which indicates a frequency-stable modulation index. For further analysis, we compute the peak phase variation from the amplitudes of the first modulation component $A(f_\mathrm{c} + f_\mathrm{m})$ and the carrier $A(f_\mathrm{c})$

$$\frac{A(f_\mathrm{c} + f_\mathrm{m})}{A(f_\mathrm{c})} = \frac{J_1(\Delta\varphi)}{J_0(\Delta\varphi)}. \tag{3}$$

The results are shown in Fig. 6 and indicate that the phase variation remains very constant up to $f_\mathrm{m} = 50\,\mathrm{MHz}$ and the maximum deviation is about $8°$ up to $1\,\mathrm{GHz}$. The lower peak phase variation $\Delta\varphi$ at $f_\mathrm{c} = 30\,\mathrm{GHz}$ is well predicted by the static phase (Fig. 4a).

Finally, we investigate the linearity of the phase modulator in terms of the modulation power $P_\mathrm{m} = \frac{\hat{V}_\mathrm{m}^2}{2*50}$ for a $f_\mathrm{m} =$

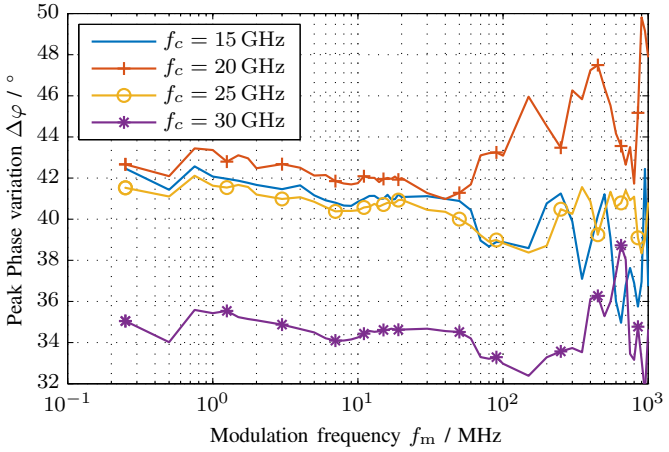

Fig. 6. Peak deviation for a modulation power $P_\mathrm{m} = -5\,\mathrm{dBm}$ for four different carrier frequencies.

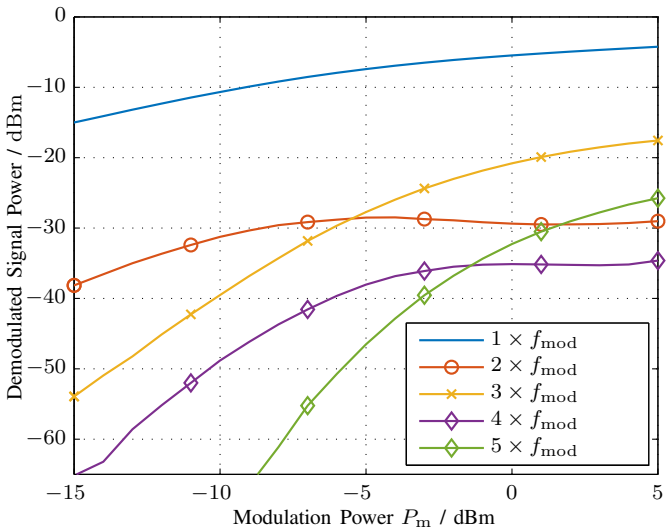

Fig. 7. Demodulated signal linearity in terms of harmonic power for a carrier frequency of $f_\mathrm{c} = 20\,\mathrm{GHz}$ and a modulation frequency $f_\mathrm{m} = 10\,\mathrm{MHz}$).

10 MHz modulation signal. The VSA is used to capture a complex time domain signal with 140 MHz of bandwidth. This signal is demodulated in postprocessing with an ideal phase detector, and the the power of the harmonics are plotted in Fig. 7, where the total power was normalized at $P_\mathrm{m} = -15\,\mathrm{dBm}$. We see that for powers below $-5\,\mathrm{dBm}$ the harmonics produced by the phase modulator are 20 dB below the fundamental. Note that this modulation power level is sufficient to create the 40° of modulation required to compensate for the phase distortion of the K-band MMIC discussed in Section II. For higher power levels the phase modulator compresses and the power particularly of the odd harmonics increases; a sign for symmetric compression and a good choice of the dc bias point V_b.

VI. Conclusion

This paper describes a GaAs MMIC phase modulator that covers 15 to 30 GHz with a modulation bandwidth of dc to 1 GHz. The measured insertion loss across the band and across modulation settings is below 3.2 dB while maintaining a return loss larger 14 dB. Dynamic measurements show a stable peak phase variation from dc to 100 MHz with minor deviations up to 1 GHz. For a 10 MHz modulation signal with $-5\,\mathrm{dBm}$ power a peak phase variation of 42° is achieved while maintaining more than 20 dB of suppression of the modulation harmonics. This shows that this phase modulator is able to compensate the phase distortion introduced by supply modulation for K-Band PAs and signal bandwidths up to 200 MHz.

Acknowledgment

We would like to acknowledge WIN Semiconductors Corp. for providing access to their PIH1-10 process and manufacturing test chips for the ECEN 5014 special topics class at the University of Colorado Boulder.

References

[1] P. Asbeck and Z. Popovic, "ET comes of age: Envelope tracking for higher-efficiency power amplifiers," *IEEE Microw. Mag.*, vol. 17, no. 3, pp. 16–25, 2016.

[2] A. Katz, R. Gray, and R. Dorval, "Truly wideband linearization," *IEEE Microw. Mag.*, vol. 10, no. 7, pp. 20–27, 2009.

[3] C. Fager, T. Eriksson, F. Barradas, K. Hausmair, T. Cunha, and J. C. Pedro, "Linearity and efficiency in 5G transmitters: New techniques for analyzing efficiency, linearity, and linearization in a 5G active antenna transmitter context," *IEEE Microw. Mag.*, vol. 20, no. 5, pp. 35–49, 2019.

[4] T. Sowlati, Y. M. Greshishchev, and C. A. T. Salama, "Phase-correcting feedback system for class E power amplifier," *IEEE J. Solid-State Circuits*, vol. 32, no. 4, pp. 544–549, 1997.

[5] H.-M. Park, D.-H. Baek, K.-I. Jeon, and S. Hong, "A predistortion linearizer using envelope-feedback technique with simplified carrier cancellation scheme for class-A and class-AB power amplifiers," *IEEE Trans. Microw. Theory Techn.*, vol. 48, no. 6, pp. 898–904, 2000.

[6] D. Danzilio, "Advanced GaAs integration for single chip mm wave front-ends." *Microwave Journal*, vol. 61, no. 5, 2018.

[7] M. R. Duffy, G. Lasser, G. Nevett, M. Roberg, and Z. Popović, "A three-stage 18.5–24-GHz GaN-on-SiC 4 W 40% efficient MMIC PA," *IEEE J. Solid-State Circuits*, vol. 54, no. 9, pp. 2402–2410, 2019.

[8] J. Staudinger, B. Gilsdorf, D. Newman, G. Norris, G. Sadowniczak, R. Sherman, and T. Quach, "High efficiency CDMA RF power amplifier using dynamic envelope tracking technique," in *2000 IEEE MTT-S International Microwave Symposium Digest (Cat. No. 00CH37017)*, vol. 2. IEEE, 2000, pp. 873–876.

[9] N. Wolff, W. Heinrich, and O. Bengtsson, "Highly efficient 1.8-GHz amplifier with 120-MHz class-G supply modulation," *IEEE Trans. Microw. Theory Techn.*, vol. 65, no. 12, pp. 5223–5230, 2017.

[10] M. R. Duffy, G. Lasser, and Z. Popović, "Distortion mitigation for 100 and 250 MHz discrete supply modulation of a three-stage K-band MMIC PA," *International Journal of Microwave and Wireless Technologies*, vol. 12, no. 8, pp. 707–715, 2020.

[11] J. F. White, "Diode phase shifters for array antennas," *IEEE Trans. Microw. Theory Techn.*, vol. 22, no. 6, pp. 658–674, 1974.

[12] S. Haykin, *Communication systems*, 4th ed. John Wiley & Sons, 2001.